



Apelin is a positive regulator of ACE2 in failing hearts

Teruki Sato,^{1,2} Takashi Suzuki,¹ Hiroyuki Watanabe,² Ayumi Kadowaki,¹ Akiyoshi Fukamizu,³ Peter P. Liu,⁴ Akinori Kimura,⁵ Hiroshi Ito,² Josef M. Penninger,⁶ Yumiko Imai,¹ and Keiji Kuba¹

¹Department of Biological Informatics and Experimental Therapeutics, Akita University Graduate School of Medicine, Akita, Japan.

²Department of Cardiovascular and Respiratory Medicine, Akita University Graduate School of Medicine, Akita, Japan. ³Life Science Center, Tsukuba Advanced Research Alliance, University of Tsukuba, Tsukuba, Ibaraki, Japan. ⁴Heart and Stroke/Richard Lewar Centre for Excellence, Toronto General Hospital, University Health Network, University of Toronto, Toronto, Ontario, Canada. ⁵Department of Molecular Pathogenesis, Medical Research Institute, Tokyo Medical and Dental University, Tokyo, Japan. ⁶IMBA, Institute of Molecular Biotechnology of the Austrian Academy of Sciences, Vienna, Austria.

Angiotensin converting enzyme 2 (ACE2) is a negative regulator of the renin-angiotensin system (RAS), catalyzing the conversion of Angiotensin II to Angiotensin 1-7. Apelin is a second catalytic substrate for ACE2 and functions as an inotropic and cardioprotective peptide. While an antagonistic relationship between the RAS and apelin has been proposed, such functional interplay remains elusive. Here we found that ACE2 was downregulated in apelin-deficient mice. Pharmacological or genetic inhibition of angiotensin II type 1 receptor (AT1R) rescued the impaired contractility and hypertrophy of apelin mutant mice, which was accompanied by restored ACE2 levels. Importantly, treatment with angiotensin 1-7 rescued hypertrophy and heart dysfunctions of apelin-knockout mice. Moreover, apelin, via activation of its receptor, APJ, increased ACE2 promoter activity in vitro and upregulated ACE2 expression in failing hearts in vivo. Apelin treatment also increased cardiac contractility and ACE2 levels in AT1R-deficient mice. These data demonstrate that ACE2 couples the RAS to the apelin system, adding a conceptual framework for the apelin-ACE2–angiotensin 1-7 axis as a therapeutic target for cardiovascular diseases.

Introduction

Apelin is an endogenous peptide with a potent positive inotropic activity (1, 2). The physiological effects of apelin are exerted through binding to its receptor APJ, a G protein-coupled receptor that shares significant homology with the angiotensin II type 1 receptor (AT1R) (3, 4). Under pathological settings, apelin signaling regulates cardiovascular functions including blood pressure, cardiac contractility, and fluid balance (5–8). Apelin exerts load-independent positive inotropy and increases coronary blood flow by vascular dilation, thereby providing beneficial effects in failing hearts (1, 2, 8, 9). In gene-targeting studies of apelin and APJ, we and others have demonstrated that the endogenous apelin-APJ axis regulates heart contractility associated with aging, exercise, and pressure overload; in the absence of apelin or APJ expression, mutant mice show reduced contractile cardiac functions (10, 11). Ligand-independent but stretch-dependent APJ signaling has recently been shown to promote pathological cardiac hypertrophy (12). However, the precise role of endogenous apelin signaling in heart function remained elusive.

Angiotensin converting enzyme 2 (ACE2) was identified as a homolog of ACE (or ACE1). ACE2 is a negative regulator of the renin-angiotensin system (RAS), catalyzing the conversion of angiotensin II (Ang II) to angiotensin 1-7 (Ang 1-7), thereby counterbalancing ACE activity (13–15). ACE2 was identified as a regulator of heart failure (16–18), diabetic nephropathy (19, 20), acute lung injury (21, 22), the receptor for the SARS coronavirus (23, 24) and as a crucial regulator of amino acid transport in the small intestines (25). The RAS peptide Ang 1-7 counterregulates Ang II actions (26, 27) via activation of the Mas G protein-coupled

receptor (28). In addition to Ang II, apelin has also been shown to be a substrate for catalytic ACE2 activity in vitro (15). ACE2 cleaves off the C terminus amino acid phenylalanine of the apelin peptide in vitro, which is a critical residue for activating APJ receptors (15). The functional interplay between apelin and ACE2 remained, however, elusive.

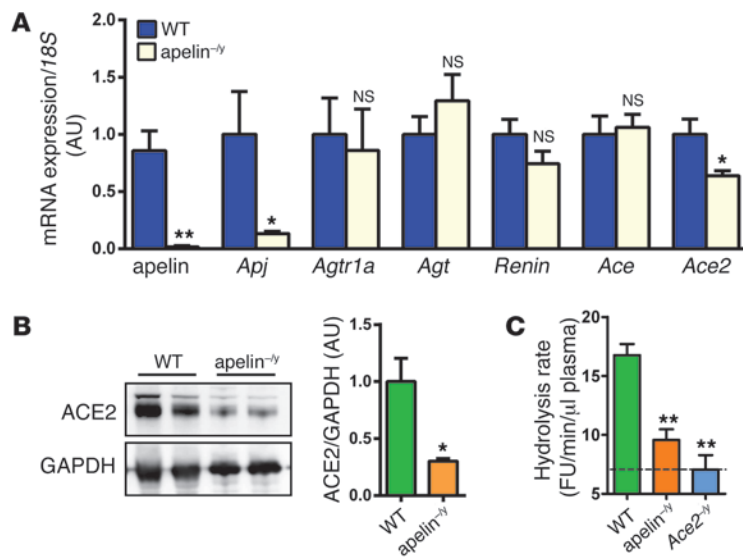
Here, we report that ACE2 expression is downregulated in apelin-knockout mice. Genetic and pharmacological inactivation of AT1R improved heart dysfunctions of apelin mutant mice. This phenotypic rescue was associated with elevated ACE2 expression. Apelin upregulated ACE2 in the failing hearts, whereas Ang 1-7 administration improved cardiac dysfunction of apelin-deficient mice in vivo. Moreover, we show that apelin-APJ increased ACE2 promoter activity and improved heart functions independently of AT1R signaling.

Results

Downregulation of ACE2 in apelin-deficient hearts. We determined expressions of key genes of the RAS in aged apelin-knockout (apelin^{-/-}) mice. mRNA expression of the apelin receptor APJ was decreased in the absence of apelin (Figure 1A), consistent with a previously reported positive feedback loop (29). Interestingly, among the RAS genes, only ACE2 mRNA expression was significantly downregulated in apelin^{-/-} mice compared with wild-type mice (Figure 1A). The protein levels of ACE2 were also markedly decreased in apelin^{-/-} mouse hearts (Figure 1B and Supplemental Figure 1A; supplemental material available online with this article; doi:10.1172/JCI69608DS1). In kidneys and intestines, other organs with high ACE2 expression (21), there were no alterations in the expression levels of ACE2 or other angiotensin-metabolizing enzymes, whereas there was a trend for ACE2 downregulation in the aorta of apelin^{-/-} mice (Supplemental Figure 1, B–D).

Conflict of interest: The authors have declared that no conflict of interest exists.

Citation for this article: *J Clin Invest.* 2013;123(12):5203–5211. doi:10.1172/JCI69608.

**Figure 1**

Downregulation of ACE2 in aged apelin-knockout mice. (A) Real-time PCR analysis for mRNA expression of apelin, APJ receptor, and the indicated renin-angiotensin component genes in the hearts of 12-month-old male apelin-knockout (apelin^{-/-}) mice and wild-type littermate mice. Values were normalized to 18S RNA ($n = 8$ per group) and are shown as mean AU. (B) Western blot for ACE2 in the hearts of apelin^{-/-} and wild-type mice. GAPDH is shown as a loading control, and representative blots and quantifications (right panels, $n = 6$) are shown. (C) ACE2 activity in the plasma of apelin^{-/-} mice. Hydrolysis rates of the fluorogenic ACE2 substrate Mca-APK-(Dnp) in the plasma of apelin^{-/-} and wild-type mice were measured at baseline with ACE2-knockout (Ace2^{-/-}) mice serving as background controls. All values represent means \pm SEM. * $P < 0.05$; ** $P < 0.01$ versus wild type.

Since ACE2 is the key enzyme generating Ang 1-7 from Ang II (16), we next measured ACE2 activity in apelin^{-/-} mice by cleavage of fluorogenic ACE2 substrate, Mca-APK-(Dnp) with ACE2-knockout (Ace2^{-/-}) mice as background controls (Figure 1C). Although there were no changes in Ang II peptide levels in apelin^{-/-} mice (not shown), which is consistent with the normal blood pressure observed in these mice (Supplemental Figure 1, E–G), plasma ACE2 activity was significantly reduced in apelin^{-/-} mice (Figure 1C). Of note, expression of other enzymes suggested to regulate Ang 1-7 formation, such as prolyl endopeptidase (30), prolyl carboxypeptidase (31), thimet oligopeptidase (32), or neprilysin (33) were not altered (Supplemental Figure 1H). Thus, loss of apelin results in downregulation of ACE2 expression and, as a consequence, potentially reduced ability to form the RAS peptide Ang 1-7.

AT1R inhibition rescues impaired heart contractility of apelin-knockout mice. Since the phenotypes of ACE2-knockout mice can be rescued by RAS inhibition (16, 17), we treated aged apelin^{-/-} mice (1 year old) with Losartan, an AT1 receptor blocker (ARB), and measured heart functions by echocardiography. After 6 weeks of ARB treatment, the impaired heart function of apelin^{-/-} mice was markedly improved to levels seen in control wild-type mice (Figure 2A and Supplemental Table 1). mRNA expression of the heart failure-associated genes brain-type natriuretic peptide (BNP) and β -myosin heavy chain (β MHC) were upregulated in aged apelin^{-/-} mouse hearts compared with wild-type controls, which was also rescued to wild-type levels upon ARB treatment (Figure 2, B and C). Thus, pharmacological AT1R inhibition reverses the aging-associated impaired heart function and altered gene expression signatures of apelin^{-/-} mice.

Consistent with our pharmacological experiments, genetic inactivation of AT1 receptors on an apelin knockout background (Agtr1a^{-/-};apelin^{-/-} mice) also rescued the decreased fractional shortening (FS) and upregulated heart failure genes of aged apelin^{-/-} mice to that of age-matched wild-type mice (Supplemental Figure 2, A–F, and Supplemental Table 2). Of note, Agtr1a^{-/-};apelin^{-/-} mice had the same levels of low blood pressure as Agtr1a^{-/-} mice (Supplemental Figure 2, G–I). To examine whether loss of AT1R also rescues pressure-induced heart failure of apelin^{-/-} mice, we subjected apelin^{-/-} mice to transverse aortic constriction (TAC).

After 8 weeks of TAC, heart functions of aged apelin-knockout mice were significantly impaired compared with wild-type mice as shown by decreased percentage of FS and enlarged systolic dimension (Figure 2, D–F, and Supplemental Table 2). Genetic inactivation of AT1R in AT1R/apelin double-mutant (Agtr1a^{-/-};apelin^{-/-}) mice rescued the impaired heart function observed in apelin^{-/-} mice (Figure 2, D–F, and Supplemental Table 2). In addition, the increased heart weight and marked fibrosis of apelin^{-/-} mice following TAC were significantly decreased in Agtr1a^{-/-};apelin^{-/-} mice (Figure 2, G and H, and Supplemental Figure 3, A and B). In line with these findings, the elevated expression of heart failure-associated (BNP, ANF, β MHC) and fibrotic (TGF β 2) genes in apelin^{-/-} mice with TAC were downregulated to the levels of control wild-type mice in the Agtr1a^{-/-};apelin^{-/-} mice (Supplemental Figure 3, C–F). Similarly, genetic inactivation of the AT1R also rescued the pressure-induced cardiac dysfunction in younger apelin^{-/-} mice (Supplemental Table 3). Therefore, cardiac dysfunction in apelin^{-/-} mice can be reversed by AT1R inactivation.

Loss of AT1 receptor upregulates ACE2 expression in apelin^{-/-} mice. We next examined whether the rescued phenotypes in apelin^{-/-} mice are associated with ACE2 expression levels. In ARB-treated apelin^{-/-} mice or mice carrying mutations in both AT1R and apelin genes (Agtr1a^{-/-};apelin^{-/-}), ACE2 mRNA expression was significantly upregulated compared with control apelin^{-/-} mice (Figure 3, A and B). In addition, the protein levels of ACE2 were also upregulated in Agtr1a^{-/-};apelin^{-/-} mice (Figure 3C). Of note, loss of AT1R resulted in increased ACE2 expression levels not only in apelin^{-/-} but also in wild-type mice (Supplemental Figure 4A). Consistently, plasma ACE2 activity was significantly elevated in Agtr1a^{-/-} mice (Supplemental Figure 4B). Thus, genetic inactivation of AT1R results in the upregulation of ACE2 expression in apelin^{-/-} mice.

Ang 1-7 rescues cardiac dysfunction and hypertrophy in apelin^{-/-} mice. Given that elevated ACE2 is functionally relevant in improving the impaired heart phenotypes of apelin^{-/-} mice, we speculated that Ang 1-7 peptide treatment should also rescue the cardiac dysfunction of apelin^{-/-} mice. Continuous infusion of Ang 1-7 with osmotic minipumps was initiated after introducing TAC-induced pressure overload in apelin^{-/-} mice, and cardiac parameters were measured after 2 weeks. The mean blood pressure was not appar-

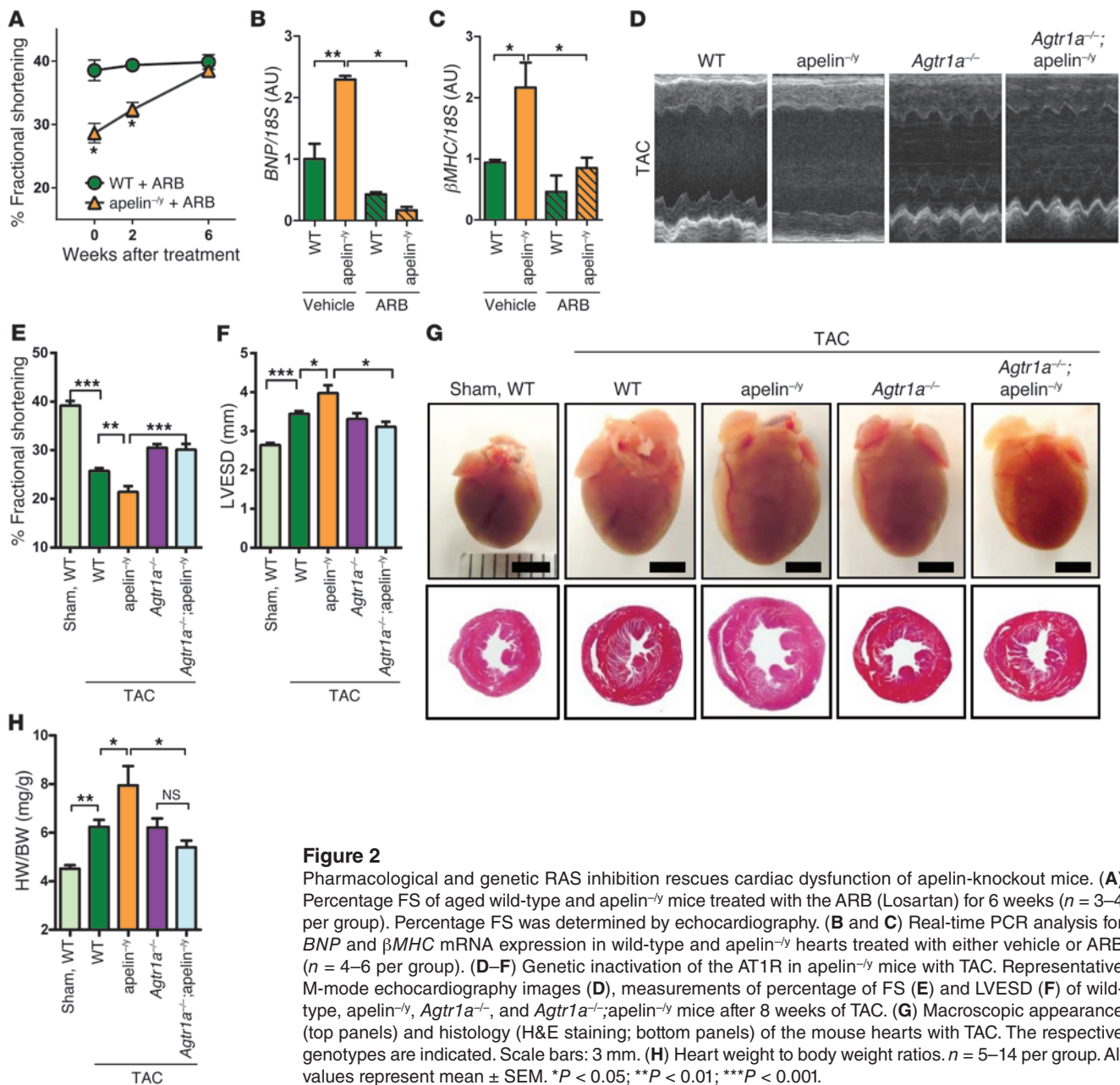


Figure 2

Pharmacological and genetic RAS inhibition rescues cardiac dysfunction of apelin-knockout mice. (A) Percentage FS of aged wild-type and apelin^{-y} mice treated with the ARB (Losartan) for 6 weeks (n = 3–4 per group). Percentage FS was determined by echocardiography. (B and C) Real-time PCR analysis for BNP and βMHC mRNA expression in wild-type and apelin^{-y} hearts treated with either vehicle or ARB (n = 4–6 per group). (D–F) Genetic inactivation of the AT1R in apelin^{-y} mice with TAC. Representative M-mode echocardiography images (D), measurements of percentage of FS (E) and LVESD (F) of wild-type, apelin^{-y}, Agtr1a^{-/-}, and Agtr1a^{-/-}; apelin^{-y} mice after 8 weeks of TAC. (G) Macroscopic appearance (top panels) and histology (H&E staining; bottom panels) of the mouse hearts with TAC. The respective genotypes are indicated. Scale bars: 3 mm. (H) Heart weight to body weight ratios. n = 5–14 per group. All values represent mean ± SEM. *P < 0.05; **P < 0.01; ***P < 0.001.

ently changed by Ang 1-7 in wild-type and apelin^{-y} mice despite lowered diastolic blood pressure in apelin^{-y} mice after treatment with Ang 1-7 (Supplemental Figure 5, A–C). Echocardiography showed that Ang 1-7 treatment did not affect FS of wild-type hearts under TAC. In contrast, in apelin^{-y} mice with TAC, decreased FS and enlarged systolic LV dimension were markedly improved by Ang 1-7 treatment (Figure 4, A–C, and Supplemental Table 4). In addition, Ang 1-7 infusions reversed the enhanced hypertrophy of apelin^{-y} mice with TAC to those of wild-type mice (Figure 4, D and E, and Supplemental Figure 5D). Similarly, elevated expression of heart failure-associated genes (BNP, βMHC, Periostin) in apelin^{-y} mice was restored to wild-type levels (Figure 4, F–H). Furthermore, decreased expression of the Ang 1-7 receptor Mas was rescued by Ang 1-7 treatment (Figure 4I). These results indicate that impaired

heart function in apelin^{-y} mice can be, at least in part, attributed to downregulation of the ACE2–Ang 1-7–Mas axis.

Apelin-APJ induces ACE2 expression in cardiomyocytes. We next asked whether exogenous apelin peptide treatment would also increase ACE2 expression. When wild-type mice were continuously treated with apelin-13 or apelin-12 peptides, ACE2 protein levels were significantly upregulated in the myocardium (Figure 5A and Supplemental Figure 6, A and B). To examine which cell types are responsible for apelin-induced ACE2 expression, we conducted ACE2 immunohistochemistry in the hearts of wild-type and apelin^{-y} mice. Prominent ACE2 staining was detected in cardiomyocytes, whereas endothelial cells expressed lower levels of ACE2 protein; this staining pattern was observed in both wild-type and mutant mice, albeit ACE2 expression was decreased in the myocardium

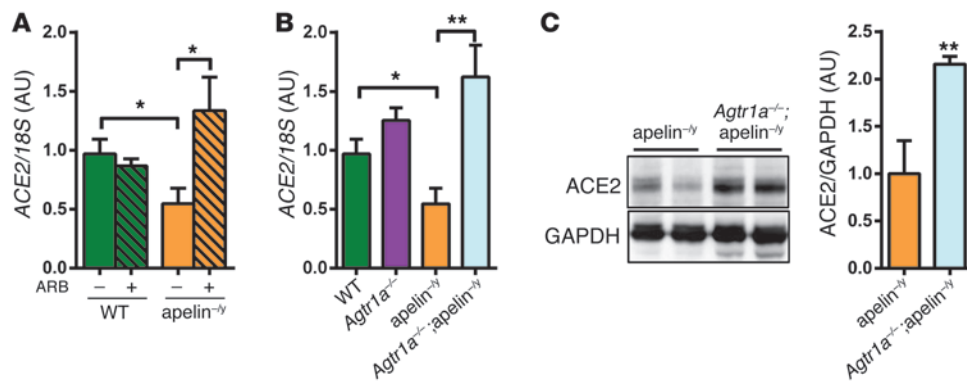


Figure 3

Inactivation of AT1R upregulates ACE2 expression in apelin-knockout mice. (A and B) Real-time PCR analysis for ACE2 mRNA expression in the hearts of ARB-treated (Losartan) apelin^{-/-} mice (A) and ARB-treated wild-type, apelin^{-/-}, Agtr1a^{-/-}, and Agtr1a^{-/-};apelin^{-/-} double mutant mice (B). (C) Western blot for ACE2 in hearts from apelin^{-/-} and Agtr1a^{-/-};apelin^{-/-} double-mutant mice. Two representative heart samples are shown for each genotype. *n* = 4–8 per group. All values represent mean ± SEM. **P* < 0.05; ***P* < 0.01.

and endothelium of apelin^{-/-} mice (Supplemental Figure 6C). Consistent with these observations, apelin-13 peptide significantly increased ACE2 expression in isolated cardiomyocytes in vitro (Figure 5B). On the other hand, ACE2 expression was not induced in coronary artery endothelial cells in vitro (not shown), a finding that remains to be explained.

To address whether apelin-APJ-mediated ACE2 expression is transcriptionally regulated, we conducted ACE2 promoter assays by using the luciferase reporter ACE2 (-1119/+103)-luc, ACE2 (-252/+103)-luc and ACE2 (-202/+103)-luc plasmids in combination with an APJ expression vector in Vero E6 cells that endogenously express ACE2. The ACE2 (-1119/+103)-luc, ACE2 (-252/+103)-luc, but not ACE2 (-202/+103)-luc constructs showed modest induction of ACE2 promoter activity (Figure 5C). Apelin dose dependently increased ACE2 (-252/+103) promoter activity (Figure 5D), an effect that was dependent on expression of the APJ receptor (Figure 5, C and E). Apelin-induced activation of ACE2 promoter was also observed in HEK293T cells (Supplemental Figure 6, D and E). Importantly, when the ACE promoter (-230/+1) reporter construct was tested under the same conditions, apelin-APJ activation did not induce the ACE promoter (Figure 5C), consistent with the downregulation of ACE2 but normal ACE expression in apelin^{-/-} mice. We further examined the role of AT1Rs on apelin-APJ-triggered ACE2 promoter activation. Coexpression of APJ and AT1R reduced ACE2 promoter activity in comparison with APJ expression alone, suggesting that AT1R antagonizes APJ (Figure 5E). On the other hand, apelin still slightly increased ACE2 promoter activity in the APJ and AT1R-coexpressing cells (Figure 5E and Supplemental Figure 6F). Taken together, activation of the apelin-APJ axis can induce ACE2 expression in vitro, which is in part dependent on AT1R expression.

Apelin upregulates ACE2 in AT1R-knockout mice. To further investigate apelin-mediated ACE2 expression, we examined the effects of apelin-13 peptides in AT1R-deficient (Agtr1a^{-/-}) mice. In wild-type mice under TAC, apelin-13 treatment improved heart functions and reduced heart weight as compared with the vehicle-treated control cohort without affecting blood pressure (Figure 6, A–D, Supplemental Figure 7, A–D, and Supplemental Table 5), consistent with previous reports (34). Interestingly, impaired heart functions as well as increased heart weights of Agtr1a^{-/-} mice under

TAC were also improved by continuous infusion of apelin-13 (Figure 6, A–D, Supplemental Figure 7D, and Supplemental Table 5). In addition, apelin-13 treatment resulted in downregulated expression of the βMHC gene in Agtr1a^{-/-} mice compared with vehicle treatment (Figure 6E). Furthermore, ACE2 expression was increased by apelin-13 peptide in Agtr1a^{-/-} mice as well as in wild-type mice (Figure 6, F and G). Thus, apelin-13 exerts cardioprotective effects in Agtr1a^{-/-} mice with TAC.

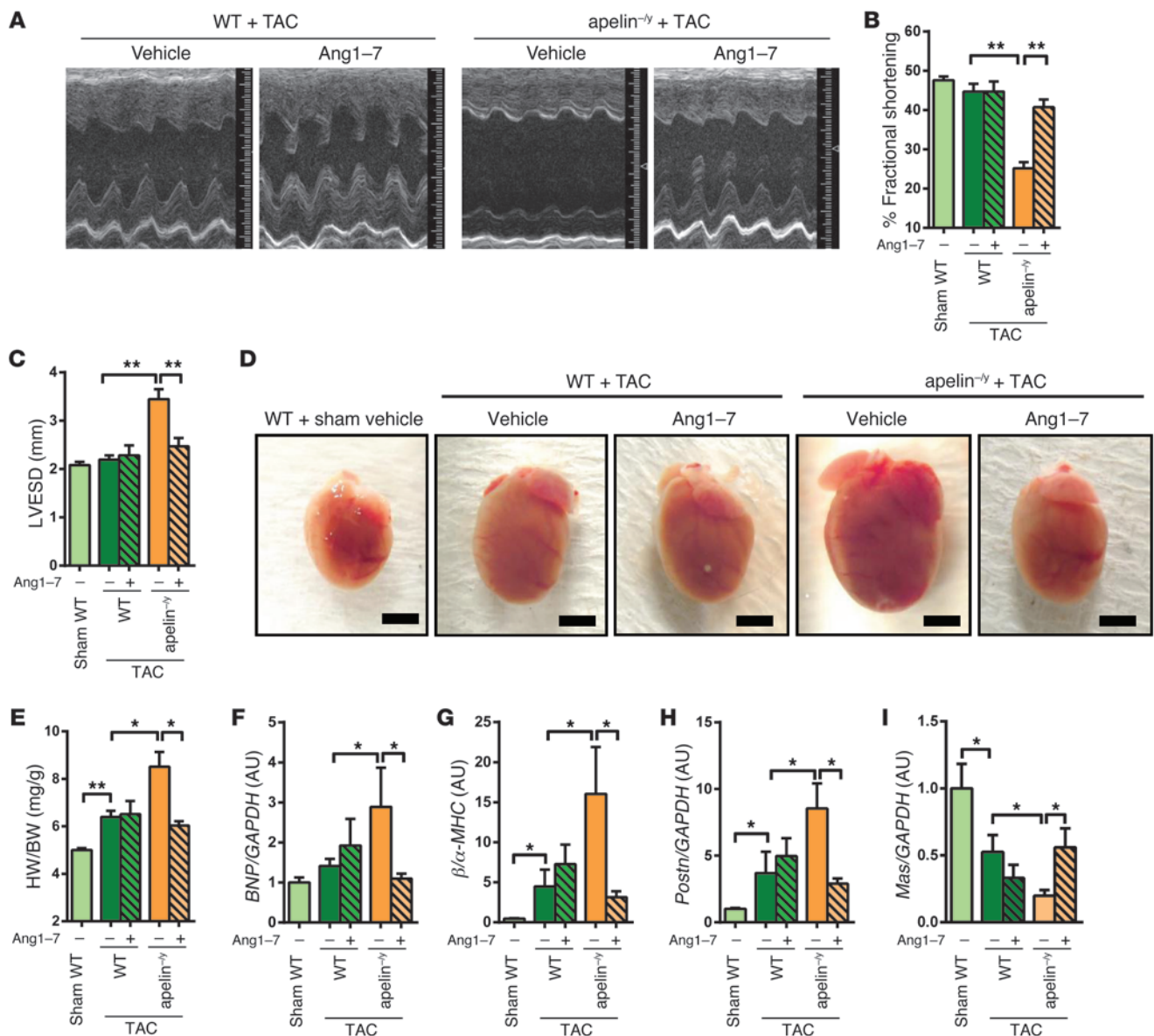
Discussion

In the current study, we report that ACE2 is downregulated in apelin-deficient mice, which

potentially impairs the ability to form Ang 1-7 peptide. Importantly, Ang 1-7 peptide treatment rescued the cardiac dysfunction in apelin mutant mice. Apelin-APJ signaling has previously been shown to counteract the effects of Ang II on AT1 receptors in defined physiologic and pathophysiologic settings. For instance, in hypertensive rat models, continuous infusion of Ang II downregulates both apelin and APJ expression (35). In addition, APJ receptors can physically interact with AT1 receptors and negatively regulate Ang II-AT1R signaling (36, 37). However, in the present study, since apelin induces ACE2 expression in the absence of AT1R, the elevation of ACE2 by apelin is likely due to transcriptional activation of ACE2 rather than antagonistic effects of apelin on Ang II-AT1R signaling.

Apelin upregulates ACE2 expression levels, as shown in this study, and antagonizes AT1R signaling via a heterodimerization of APJ and AT1R (36, 37); in both scenarios, apelin is speculated to be inactivated by ACE2 (15). The Ang 1-7–Mas receptor axis has been shown to have beneficial effects in cardiovascular diseases (27, 38). Importantly, Ang 1-7, generated by ACE2, counterregulates Ang II-AT1R signaling (26, 27). Thus, even if apelin is inactivated by ACE2, activation of the apelin-APJ-ACE2 axis is likely to lead to Ang 1-7-mediated counterregulation of the RAS. Indeed, Mas receptor expression was found to be downregulated in the hearts of apelin^{-/-} mice, which could be restored by Ang 1-7 treatment (Figure 4I), suggesting that Ang 1-7 signaling and its positive effect on Mas expression is suppressed in apelin^{-/-} hearts. Therefore, apelin appears to positively control the Ang 1-7–Mas system.

A previous study suggested that ACE2 is involved in cardiac development, whereby the ACE2 promoter is activated in epicardial cells in Xenopus embryos via a GATA-binding site (39). The GATA-binding sites in the ACE2 promoter region are conserved among species (39), and several potential GATA-binding sites, namely AGATAG (-697/-692), AGATAA (-352/-347), TTATCT (-305/-300), and TGATAA (+23/+28), exist in the human ACE2 promoter. In our reporter assays in Vero E6 cells, we uncovered the -252/-202 region to be required for apelin-induced ACE2 activation. This region contains a binding site for hepatocyte nuclear factor 1-β (HNF1-β), suggesting a role for HNF1-β. However, the minimal ACE2 promoter (-202/+103) was activated by apelin in

**Figure 4**

Ang 1-7 rescues impaired heart function in apelin-knockout mice. (A–C) Heart function measurements. Representative M-mode echocardiography images (A), measurements of percentage of FS (B), and LVESD (C) of sham- or TAC-operated wild-type and apelin^{-/-} mice treated with Ang 1-7 or vehicle for 2 weeks. (D and E) Rescue of TAC-induced cardiac hypertrophy by Ang 1-7. Macroscopic images of hearts (D) and heart weight to body weight ratios (E) of wild-type and apelin^{-/-} mice treated with Ang 1-7 or vehicle control. Scale bars: 3 mm. (F–I) Real-time PCR analysis for *BNP*, β MHC, Periostin (*Postn*), and Mas receptor (*Mas*) mRNA expression in the hearts of sham- or TAC-operated wild-type and apelin^{-/-} mice receiving Ang 1-7 or vehicle. Data are normalized to GAPDH mRNA levels. $n = 5$ –10 per group. All values represent mean \pm SEM. * $P < 0.05$; ** $P < 0.01$.

HEK293 cells, i.e., in the absence of HNF1- β binding, and there have been no reports that HNF1- β has a role in the cardiovascular system. Thus, the significance of HNF1- β remains unclear. On the other hand, various GATA family members previously reported to control endothelial tissue development (GATA-2/3) and cardiac function (GATA-4/5/6) have been implicated in ACE2 upregulation (40). Indeed, the apelin-APJ activation pathway has been shown to contribute to the differentiation of cardiac and endothelial progenitor cells in various animal models, e.g., loss of apelin in zebrafish results in severe defects of heart field for-

mation (41–44). Moreover, non-cell autonomous activation of GATA5/Smarcd3b has recently been suggested to be downstream of apelin signaling in cardiac development (45), further indicating that GATA5 is involved in the induction of ACE2 expression. Since our study shows that ACE2 promoter activity is induced by apelin, apelin signaling may also induce ACE2 in developing hearts, warranting further studies on the role of the apelin-ACE2 axis in the development of the cardiovascular system.

In conclusion, our genetic data demonstrate a mode of cross-talk between the apelin and the RASs in controlling cardiac con-

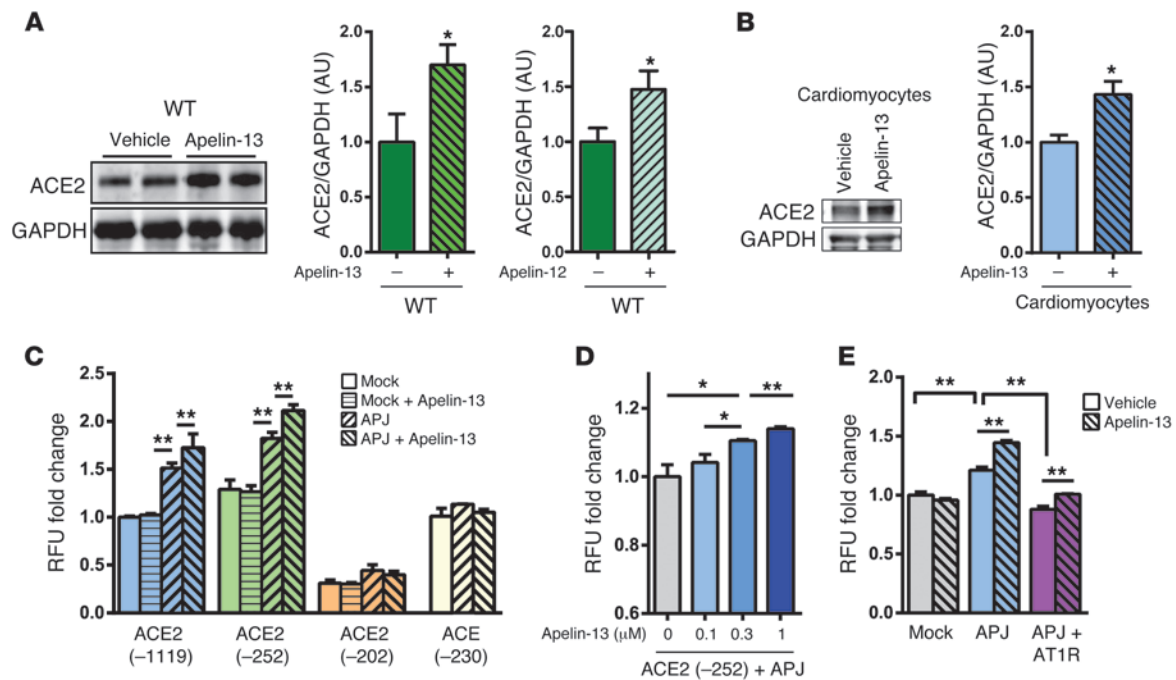


Figure 5

Apelin upregulates ACE2 expression in vivo and in vitro. **(A)** Western blot for ACE2 in the hearts of mice infused with apelin-13 or apelin-12. Hearts were harvested after 2 weeks of apelin peptide infusions. Bar graphs show quantifications ($n = 4-6$ per group). **(B)** ACE2 expression in primary cardiomyocytes isolated from wild-type mice treated with either vehicle or apelin-13 peptides ($1 \mu\text{M}$) for 24 hours. **(C)** ACE2 promoter assay using the luciferase reporter plasmids ACE2 (-1119/+103)-luc, ACE2 (-252/+103)-luc, ACE2 (-202/+103)-luc, or ACE2 (-230/+1)-luc in combination with APJ expression vectors in Vero E6 cells. Cells were either left untreated or treated with $1 \mu\text{M}$ apelin-13 peptide (apelin-13). **(D)** Dose dependency of apelin on ACE2 promoter activation in Vero E6 cells. **(E)** Effects of AT1R expression on apelin-induced ACE2 promoter (-252/+103) activity in HEK293T cells transfected with control mock vectors (Mock), APJ expression vectors (APJ), or a combination of APJ and AT1R vectors (APJ + AT1R) and treated with or without apelin-13. $n = 3$ per group in at least 2 independent experiments. All values represent mean \pm SEM. * $P < 0.05$; ** $P < 0.01$.

tractility and heart failure. This crosstalk is established via ACE2. The RAS is one of the major targets to treat chronic heart failure patients in the clinic (46). Both ACE2 and apelin exhibit beneficial effects in the cardiovascular system, and recombinant ACE2 protein has recently been shown as a candidate therapeutic for treating heart failure in animal models (47). The ACE2-coupled crosstalk between the RAS and the apelin system provides an important mechanistic insight into heart failure and may lead to the development of new therapeutic regimens.

Methods

Mice. Apelin-knockout (apelin^{-/-}), ACE2-knockout (Ace2^{-/-}), and AT1 receptor-knockout (Agtr1a^{-/-}) mice were generated as described (10, 48) and backcrossed to C57BL/6J mice more than 10 generations. Double-mutant mice carrying mutations in both AT1 receptors and apelin (Agtr1a^{-/-}; apelin^{-/-} mice) were generated and maintained on a C57BL/6J background. Mice were genotyped by PCR and Southern blotting and maintained at the animal facilities of Akita University Graduate School of Medicine.

Pharmacological interventions. For ARB treatment, 12-month-old wild-type and littermate apelin^{-/-} male mice received either vehicle or the ARB Losartan (0.6 g/l; LKT Laboratories Inc.) in their drinking water. At 2 and 6 weeks after treatment, echocardiography was performed and the mice were sacrificed for analysis. For Ang 1-7 treatment, wild-type and apelin^{-/-} male mice were subcutaneously infused with either saline or Ang 1-7 (Sigma-Aldrich) at 1 mg/kg/d for 2 weeks by osmotic minipumps (Alzet

model 1002; Alza Corp.) after TAC operation. For apelin peptide treatment, wild-type and Agtr1a^{-/-} male mice underwent sham or TAC surgeries, and were infused with either saline, apelin-12 (BEX), or apelin-13 (BEX) at 1 mg/kg/d by osmotic pump. Two weeks after treatment, echocardiography was performed and mice sacrificed.

TAC. Six-month-old control wild-type, apelin^{-/-}, Agtr1a^{-/-}, Agtr1a^{-/-}; apelin^{-/-}, and Ace2^{-/-} littermate mice were subjected to pressure overload by TAC as previously described (10). Briefly, mice were anesthetized via intraperitoneal injection of ketamine (100 mg/kg) and xylazine (20 mg/kg), and a longitudinal incision of 2-3 mm was then made in the proximal portion of sternum, visualizing the aortic arch in supine position. The aortic arch was ligated between the brachiocephalic and left common carotid arteries with an overlying 27-gauge needle by 7-0 silk. The needle was immediately removed, leaving a discrete region of constriction. The sham surgery-treated group underwent a similar procedure without ligation. Echocardiography was performed 2 weeks or 8 weeks after TAC or sham surgery and mice were then sacrificed.

Echocardiography and blood pressure measurements. Echocardiographic measurements were performed as described (10). Briefly, mice were anesthetized with isoflurane (1%)/oxygen, and echocardiography was performed using Vevo770 equipped with a 30-MHz linear transducer. FS was calculated as follows: FS = [(LVEDD - LVESD)/LVEDD] \times 100, where LVEDD indicates LD end-diastolic diameter and LVESD indicates LV end-systolic diameter. We used 2D-guided M-mode measurements to determine percentage FS. The heart was first imaged in 2D mode in the parasternal

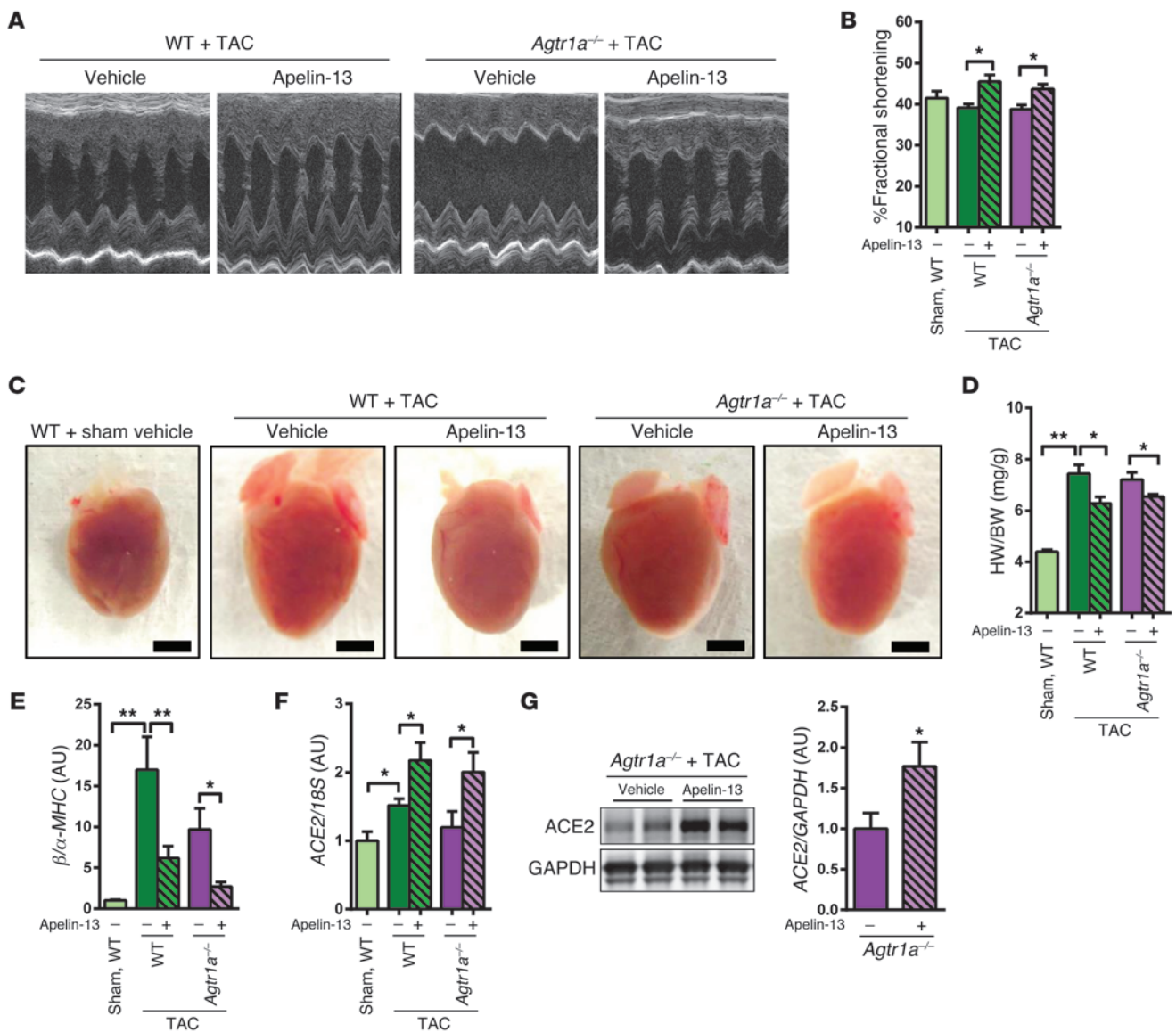


Figure 6

AT1R-independent effects of apelin on ACE2 induction. (A–C) Heart function measurements. Representative M-mode echocardiography images (A) and measurements of percentage of FS (B) of TAC- or sham-treated wild-type and *Agtr1a*^{-/-} mice receiving apelin-13 or vehicle for 2 weeks. (C and D) Reduction of cardiac hypertrophy in TAC-treated *Agtr1a*^{-/-} mice by apelin-13. Macroscopic heart images (C) and heart weight to body weight ratios (D) of wild-type and *Agtr1a*^{-/-} mice treated with apelin-13 or vehicle. *n* = 5–6 per group. Scale bars: 3 mm. (E and F) Real-time PCR analysis for mRNA expression of β MHC (E) and ACE2 (F) of TAC- or sham-treated wild-type and *Agtr1a*^{-/-} mice receiving apelin-13 or vehicle for 2 weeks. (G) Western blot for ACE2 in total protein lysates from hearts of *Agtr1a*^{-/-} mice treated with vehicle and apelin-13 under TAC. *n* = 8–11 per group. Right panel shows quantification of ACE2 protein expression normalized to GAPDH. All values represent mean \pm SEM. **P* < 0.05; ***P* < 0.01.

short-axis view. From this view, an M-mode cursor was positioned perpendicularly to the interventricular septum and posterior wall of the LV at the level of the papillary muscles. M-mode images were obtained for measurement of wall thickness and chamber dimensions with the use of the leading-edge convention adapted by the American Society of Echocardiography. Blood pressure was measured in conscious mice by a programmable sphygmomanometer (BP-200; Softron) using the tail-cuff method after 5 days of daily training, as described previously (49).

Histology. Heart tissues were fixed with 4% formalin and embedded in paraffin. Then 5- μ m-thick sections were prepared and stained with H&E or Masson-Trichrome. For measurements of fibrotic area, images of heart sections

stained with Masson-Trichrome were taken using a BIOREVO microscope (BZ9000; Keyence) and analyzed using the BZII analyzer software (Keyence).

Quantitative real-time PCR. RNA was extracted using TRIzol reagent (Invitrogen) and cDNA synthesized using the PrimeScript RT reagent kit (TAKARA). Sequences of the forward and reverse primers of the genes studied are shown in Supplemental Table 6. Real-time PCR was run in 96-well plates using a SYBR Premix ExTaq II (TAKARA) according to the instructions of the manufacturer. Relative gene expression levels were quantified using Thermal Cycler Dice Real Time System II software (TAKARA).

Western blotting. Heart protein was extracted using a TNE lysis buffer (50 mM Tris, 150 mM NaCl, 1 mM EDTA, 1% NP40, protease inhibitor (Com-



plete Mini; Roche), 100 mM NaF, 2 mM Na₃VO₄) and Microsmash (MS-100R, TOMY). After sonication and denaturation with LDS sample buffer (Invitrogen) at 70 °C, proteins were electrophoresed on NuPAGE bis-tris precast gels (Invitrogen) and transferred to nitrocellulose membranes (0.2 mm pore; Invitrogen). Anti-ACE2 antibodies (16), the specificity of which was confirmed on tissues from *Ace2*^{-/-} mice (Supplemental Figure 1A), were used as described, and the bands visualized with ECL reagent (GE Healthcare) using Image Quant LAS4000 (GE Healthcare). Image Quant TL software was used for quantification of bands.

ACE2 enzymatic activity measurements. ACE2 activity in plasma was measured by catalytic cleavage of the fluorogenic substrate Mca-APK-(Dnp) (Anaspec) as described previously (21). Briefly, heparinized plasma was diluted with assay buffer, reactions were performed without any inhibitors at 37 °C for 1 hour, and fluorescence was measured using an Infinite M200Pro (TECAN) plate reader at an excitation wavelength of 330 nm and an emission wavelength of 390 nm. Hydrolysis rates were quantified as fluorescence units/min/amount/volume of plasma.

Luciferase reporter assays. Vero E6 cells or HEK293T cells were seeded in 24-well plates (1.0 × 10⁵ cells/well). Cells were transfected with 100 ng of APJ plasmid, 100 ng of AT1R plasmid (50), 300 ng of ACE2 promoter (51), or ACE promoter (52), reporter plasmids, and 100 ng of renilla-luciferase plasmid using Lipofectamine 2000 (Invitrogen) 12 hours before treatment. Eight hours after addition of 1 μM of apelin and/or 1 μM Ang II, cells were washed with D-PBS (Invitrogen) once, lysed with lysis reagent included in the Dual-Luciferase Assay System kit (Promega), and then luciferase assays were performed according to the manufacturer's instructions. Luciferase activity was measured using the GloMAX-Multi Detection System (Promega). The ACE2-luciferase reporter plasmids containing the 1119-bp, 252-bp, and 202-bp proximal human ACE2 promoter regions have been described previously (51).

Primary cardiomyocyte cultures. Primary cardiomyocytes were isolated from prenatal mouse hearts of wild-type mice as described previously (53). Briefly, hearts were excised and rapidly minced into 3 or 4 pieces in MSS buffer (30 mM HEPES, 120 mM NaCl, 4 mM glucose, 2 mM KCl, 1 mM KH₂PO₄, pH 7.6). After digestion with collagenase (Wako) for 45 minutes at 35 °C, cardiomyocytes were collected, preplated to exclude noncardiomyocytes, and plated on gelatinized culture dishes or plates

with DMEM/F-12 (Gibco; Invitrogen) supplemented with 10% fetal bovine serum (Equitech Bio). Cardiomyocytes were cultured in 24-well plates, treated with 1 μM apelin, and protein samples were extracted as described above for Western blotting.

Statistics. Data are presented as mean values ± SEM. Normally distributed data were analyzed by an unpaired 2-tailed *t* test. Data not normally distributed were analyzed using the Mann-Whitney test. *P* < 0.05 was considered significant.

Study approval. All animal experiments conformed to the *Guide for the care and use of laboratory animals* (NIH publication no. 85-23. Revised 1996). Approval for the experiments was granted by the ethics review board of Akita University.

Acknowledgments

We thank all members of our laboratories for technical assistance and helpful discussions. This work was supported in part by the Joint Usage/Research Program of Medical Research Institute, Tokyo Medical and Dental University. K. Kuba is supported by Funding Program for the Next Generation of World-Leading Researchers from the Japan Society for the Promotion of Science, the Kaken (22390155) from the Japanese Ministry of Science, and the Inamori Foundation. Y. Imai is supported by Funding Program for the Next Generation of World-Leading Researchers from the Japan Society for the Promotion of Science. J.M. Penninger is supported by IMBA, the Austrian National Bank, the Austrian Ministry of Science and Education, and an EU Advanced ERC grant. This work is supported by the Joint Usage/Research Program of Medical Research Institute, Tokyo Medical and Dental University.

Received for publication March 1, 2013, and accepted in revised form August 29, 2013.

Address correspondence to: Keiji Kuba, Department of Biological Informatics and Experimental Therapeutics, Akita University Graduate School of Medicine, 1-1-1 Hondo, Akita 010-8543, Japan. Phone: 81.18.884.6067; Fax: 81.18.836.2603; E-mail: kuba@med.akita-u.ac.jp.

1. Szokodi I, et al. Apelin, the novel endogenous ligand of the orphan receptor APJ, regulates cardiac contractility. *Circ Res*. 2002;91(5):434–440.
2. Berry MF, et al. Apelin has in vivo inotropic effects on normal and failing hearts. *Circulation*. 2004;110(11 suppl 1):II187–II193.
3. O'Dowd BF, et al. A human gene that shows identity with the gene encoding the angiotensin receptor is located on chromosome 11. *Gene*. 1993; 136(1–2):355–360.
4. Tatemoto K, et al. Isolation and characterization of a novel endogenous peptide ligand for the human APJ receptor. *Biochem Biophys Res Commun*. 1998; 251(2):471–476.
5. Lee DK, et al. Characterization of apelin, the ligand for the APJ receptor. *J Neurochem*. 2000;74(1):34–41.
6. Reaux A, et al. Physiological role of a novel neuropeptide, apelin, and its receptor in the rat brain. *J Neurochem*. 2001;77(4):1085–1096.
7. Chen MM, et al. Novel role for the potent endogenous inotropic apelin in human cardiac dysfunction. *Circulation*. 2003;108(12):1432–1439.
8. Ashley EA, et al. The endogenous peptide apelin potentially improves cardiac contractility and reduces cardiac loading in vivo. *Cardiovasc Res*. 2005; 65(1):73–82.
9. Japp AG, et al. Acute cardiovascular effects of apelin in humans: potential role in patients with chronic heart failure. *Circulation*. 2010;121(16):1818–1827.
10. Kuba K, et al. Impaired heart contractility in Apelin gene-deficient mice associated with aging and pressure overload. *Circ Res*. 2007;101(4):e32–e42.
11. Charo DN, et al. Endogenous regulation of cardiovascular function by apelin-APJ. *Am J Physiol Heart Circ Physiol*. 2009;297(5):H1904–H1913.
12. Scimia MC, et al. APJ acts as a dual receptor in cardiac hypertrophy. *Nature*. 2012;488(7411):394–398.
13. Donoghue M, et al. A novel angiotensin-converting enzyme-related carboxypeptidase (ACE2) converts angiotensin I to angiotensin 1-9. *Circ Res*. 2000;87(5):E1–E9.
14. Tipnis SR, Hooper NM, Hyde R, Karran E, Christie G, Turner AJ. A human homolog of angiotensin-converting enzyme. Cloning and functional expression as a captopril-insensitive carboxypeptidase. *J Biol Chem*. 2000;275(43):33238–33243.
15. Vickers C, et al. Hydrolysis of biological peptides by human angiotensin-converting enzyme-related carboxypeptidase. *J Biol Chem*. 2002; 277(17):14838–14843.
16. Crackower MA, et al. Angiotensin-converting enzyme 2 is an essential regulator of heart function. *Nature*. 2002;417(6891):822–828.
17. Yamamoto K, et al. Deletion of angiotensin-converting enzyme 2 accelerates pressure overload-induced cardiac dysfunction by increasing local angiotensin II. *Hypertension*. 2006;47(4):718–726.
18. Oudit GY, et al. Angiotensin II-mediated oxidative stress and inflammation mediate the age-dependent cardiomyopathy in ACE2 null mice. *Cardiovasc Res*. 2007;75(1):29–39.
19. Oudit GY, et al. Loss of angiotensin-converting enzyme-2 leads to the late development of angiotensin II-dependent glomerulosclerosis. *Am J Pathol*. 2006;168(6):1808–1820.
20. Tikellis C, et al. ACE2 deficiency modifies renoprotection afforded by ACE inhibition in experimental diabetes. *Diabetes*. 2008;57(4):1018–1025.
21. Imai Y, et al. Angiotensin-converting enzyme 2 protects from severe acute lung failure. *Nature*. 2005;436(7047):112–116.
22. Kuba K, Imai Y, Ohto-Nakanishi T, Penninger JM. Trilogy of ACE2: a peptidase in the renin-angiotensin system, a SARS receptor, and a partner for amino acid transporters. *Pharmacol Ther*. 2010; 128(1):119–128.
23. Li W, et al. Angiotensin-converting enzyme 2 is a functional receptor for the SARS coronavirus. *Nature*. 2003;426(6965):450–454.
24. Kuba K, et al. A crucial role of angiotensin converting enzyme 2 (ACE2) in SARS coronavirus-induced lung injury. *Nat Med*. 2005;11(8):875–879.
25. Hashimoto T, et al. ACE2 links amino acid malnutrition to microbial ecology and intestinal inflammation. *Nature*. 2012;487(7408):477–481.
26. Ferrario CM, Chappell MC, Tallant EA, Brosnihan KB, Diz DI. Counterregulatory actions of angioten-



- sin-(1-7). *Hypertension*. 1997;30(3 pt 2):535–541.
27. Ferreira AJ, et al. Therapeutic implications of the vasoprotective axis of the renin-angiotensin system in cardiovascular diseases. *Hypertension*. 2010; 55(2):207–213.
28. Santos RA, et al. Angiotensin-(1-7) is an endogenous ligand for the G protein-coupled receptor Mas. *Proc Natl Acad Sci U S A*. 2003;100(14):8258–8263.
29. McLean DL, et al. Apelin/APJ signaling is a critical regulator of statin effects in vascular endothelial cells – brief report. *Arterioscler Thromb Vasc Biol*. 2012;32(11):2640–2643.
30. Nozaki Y, Sato N, Iida T, Hara K, Fukuyama K, Epstein WL. Prolyl endopeptidase purified from granulomatous inflammation in mice. *J Cell Biochem*. 1992;49(3):296–303.
31. Ody CE, Marinkovic DV, Hammon KJ, Stewart TA, Erdos EG. Purification and properties of prolylcarboxypeptidase (angiotensinase C) from human kidney. *J Biol Chem*. 1978;253(17):5927–5931.
32. Chappell MC, Gomez MN, Pirro NT, Ferrario CM. Release of angiotensin-(1-7) from the rat hindlimb: influence of angiotensin-converting enzyme inhibition. *Hypertension*. 2000;35(1 pt 2):348–352.
33. Yamamoto K, Chappell MC, Brosnihan KB, Ferrario CM. In vivo metabolism of angiotensin I by neutral endopeptidase (EC 3.4.24.11) in spontaneously hypertensive rats. *Hypertension*. 1992; 19(6 pt 2):692–696.
34. Foussal C, et al. Activation of catalase by apelin prevents oxidative stress-linked cardiac hypertrophy. *FEBS Lett*. 2010;584(11):2363–2370.
35. Iwanaga Y, Kihara Y, Takenaka H, Kita T. Down-regulation of cardiac apelin system in hypertrophied and failing hearts: Possible role of angiotensin II-angiotensin type 1 receptor system. *J Mol Cell Cardiol*. 2006;41(5):798–806.
36. Chun HJ, et al. Apelin signaling antagonizes Ang II effects in mouse models of atherosclerosis. *J Clin Invest*. 2008;118(10):3343–3354.
37. Siddiquee K, Hampton J, McAnally D, May L, Smith L. The apelin receptor inhibits the angiotensin II type 1 receptor via allosteric trans-inhibition. *Br J Pharmacol*. 2013;168(5):1104–1117.
38. Santos RA, Ferreira AJ, Verano-Braga T, Bader M. Angiotensin-converting enzyme 2, angiotensin-(1-7) and Mas: new players of the renin-angiotensin system. *J Endocrinol*. 2013;216(2):R1–R17.
39. Chou CF, et al. ACE2 orthologues in non-mammalian vertebrates (Danio, Gallus, Fugu, Tetraodon and Xenopus). *Gene*. 2006;377:46–55.
40. Jiang Y, Evans T. The Xenopus GATA-4/5/6 genes are associated with cardiac specification and can regulate cardiac-specific transcription during embryogenesis. *Dev Biol*. 1996;174(2):258–270.
41. Inui M, Fukui A, Ito Y, Asashima M. Xapelin and Xmsr are required for cardiovascular development in *Xenopus laevis*. *Dev Biol*. 2006;298(1):188–200.
42. Scott IC, et al. The g protein-coupled receptor agr11b regulates early development of myocardial progenitors. *Dev Cell*. 2007;12(3):403–413.
43. Zeng XX, Wilm TP, Sepich DS, Solnica-Krezel L. Apelin and its receptor control heart field formation during zebrafish gastrulation. *Dev Cell*. 2007; 12(3):391–402.
44. Red-Horse K, Ueno H, Weissman IL, Krasnow MA. Coronary arteries form by developmental reprogramming of venous cells. *Nature*. 2010;464(7288):549–553.
45. Paskaradevan S, Scott IC. The Aplnr GPCR regulates myocardial progenitor development via a novel cell-non-autonomous, Galpha(i/o) protein-independent pathway. *Biol Open*. 2012;1(3):275–285.
46. Gersh BJ, et al. 2011 ACCF/AHA guideline for the diagnosis and treatment of hypertrophic cardiomyopathy: executive summary: a report of the American College of Cardiology Foundation/American Heart Association Task Force on Practice Guidelines. *Circulation*. 2011;124(24):2761–2796.
47. Zhong J, et al. Angiotensin-converting enzyme 2 suppresses pathological hypertrophy, myocardial fibrosis, and cardiac dysfunction. *Circulation*. 2010;122(7):717–728.
48. Sugaya T, et al. Angiotensin II type 1a receptor-deficient mice with hypotension and hyperreninemia. *J Biol Chem*. 1995;270(32):18719–18722.
49. Ishida J, et al. Regulatory roles for APJ, a seven-transmembrane receptor related to angiotensin-type 1 receptor in blood pressure in vivo. *J Biol Chem*. 2004;279(25):26274–26279.
50. Nishida M, et al. G alpha 12/13- and reactive oxygen species-dependent activation of c-Jun NH2-terminal kinase and p38 mitogen-activated protein kinase by angiotensin receptor stimulation in rat neonatal cardiomyocytes. *J Biol Chem*. 2005; 280(18):18434–18441.
51. Senkel S, Lucas B, Klein-Hitpass L, Ryffel GU. Identification of target genes of the transcription factor HNF1beta and HNF1alpha in a human embryonic kidney cell line. *Biochim Biophys Acta*. 2005; 1731(3):179–190.
52. Day RM, et al. Hepatocyte growth factor regulates angiotensin converting enzyme expression. *J Biol Chem*. 2004;279(10):8792–8801.
53. Yuki K, et al. Mitochondrial dysfunction increases expression of endothelin-1 and induces apoptosis through caspase-3 activation in rat cardiomyocytes in vitro. *J Cardiovasc Pharmacol*. 2000; 36(5 suppl 1):S205–S208.